The Astrophysical Journal Letters, 781:L27 (6pp), 2014 February 1 doi:10.1088/2041-8205/781/2/L27

PROTON KINETIC EFFECTS IN VLASOV AND SOLAR WIND TURBULENCE

S. Servidio[1], K. T. Osman[2], F. Valentini[1], D. Perrone[1], F. Califano[3], S. Chapman[2,4,5], W. H. Matthaeus[6], and P. Veltri[1]
[1] Dipartimento di Fisica, Università della Calabria, I-87036 Cosenza, Italy; sergio.servidio@fis.unical.it
[2] Centre for Fusion, Space and Astrophysics, University of Warwick, Coventry, CV4 7AL, UK
[3] Dipartimento di Fisica and CNISM, Università di Pisa, I-56127 Pisa, Italy
[4] Max Planck Institute for the Physics of Complex Systems, D-01187 Dresden, Germany
[5] Department of Mathematics and Statistics, University of Tromso, NO-9037 Tromso, Norway
[6] Bartol Research Institute and Department of Physics and Astronomy, University of Delaware, Newark, DE 19716, USA
Received 2013 November 14; accepted 2013 December 21; published 2014 January 9

ABSTRACT

Kinetic plasma processes are investigated in the framework of solar wind turbulence, employing hybrid Vlasov–Maxwell (HVM) simulations. Statistical analysis of spacecraft observation data relates proton temperature anisotropy $T_\perp/T_\parallel$ and parallel plasma beta $\beta_\parallel$, where subscripts refer to the ambient magnetic field direction. Here, this relationship is recovered using an ensemble of HVM simulations. By varying plasma parameters, such as plasma beta and fluctuation level, the simulations explore distinct regions of the parameter space given by $T_\perp/T_\parallel$ and $\beta_\parallel$, similar to solar wind sub-datasets. Moreover, both simulation and solar wind data suggest that temperature anisotropy is not only associated with magnetic intermittent events, but also with gradient-type structures in the flow and in the density. This connection between non-Maxwellian kinetic effects and various types of intermittency may be a key point for understanding the complex nature of plasma turbulence.

Key words: magnetic fields – plasmas – solar wind – turbulence

Online-only material: color figures

1. INTRODUCTION

Magnetohydrodynamic turbulence forms small scale coherent structures that may be sites of enhanced dissipation (Matthaeus & Montgomery 1980; Veltri 1999), magnetic reconnection, and plasma heating (Parker 1988; Marsch 2006). However, in low-collisionality plasmas such as the solar wind, one expects to find kinetic processes including temperature anisotropy and energization of suprathermal particles at small scales (Marsch 2006; Gary 1993). Given this duality, there are many open questions regarding how a turbulent plasma such as the solar wind dissipates large scale energy and how observed microscopic non-equilibrium conditions are related to the dynamics and thermodynamics that control large scale features. At stake are issues such as the physical basis for acceleration of the solar wind itself (Verdini et al. 2010).

Recently, there has been intensive activity in understanding the organization of solar wind plasma (Kasper et al. 2002; Hellinger et al. 2006; Bale et al. 2009; Maruca et al. 2011) and, in particular, the distribution and evolution of solar wind parcels in a plane described by the parallel plasma beta and the proton temperature anisotropy have attracted intensive interest. The general trend with wind expansion toward lower anisotropy and higher parallel beta is understood from adiabatic theory (Hellinger et al. 2006; Matteini et al. 2007), while the limiting behavior may be associated with instabilities (Hellinger et al. 2006; Bale et al. 2009; Maruca et al. 2011) and other processes that may preferentially operate in coherent structures (Greco et al. 2008; Osman et al. 2011, 2012b). So far, there has been no theoretical model that explains why the solar wind plasma occupies a wide and distinctive range of these parameters. Here we explore the connections between solar wind kinetic properties and turbulence, employing Vlasov kinetic simulations. We are able to recover the distinctive distribution of solar wind kinetic parameters through the combined effects of variation in the initial parameters along with the natural dynamical variations due to the turbulence itself. Therefore, we suggest that the kinetic properties of an ensemble of solar wind observations is controlled by turbulence properties.

In situ spacecraft measurements reveal that interplanetary proton velocity distribution functions (VDFs) are anisotropic with respect to the magnetic field (Marsch et al. 1982, 2004). Values of the anisotropy $T_\perp/T_\parallel$ range broadly, with most values between 10^{-1} and 10 (Bale et al. 2009; Maruca et al. 2011). The distribution of $T_\perp/T_\parallel$ depends systematically on the ambient proton parallel beta $\beta_\parallel = n_p k_B T_\parallel/(B^2/2\mu_0)$—the ratio of parallel kinetic pressure to magnetic pressure, manifesting a characteristic shape in the parameter plane defined by $T_\perp/T_\parallel$ and $\beta_\parallel$ (Kasper et al. 2002; Bale et al. 2009; Maruca et al. 2011). More recently (Osman et al. 2012a), observations have suggested that a link exists between anisotropy and intermittent current sheets. The latter study employed the Partial Variance of Increments (PVI) technique which provides a running measure of the magnetic field intermittency level, and is able to quantify the presence of strong discontinuities (Greco et al. 2008). Elevated PVI values signal an increased likelihood of finding coherent magnetic structures such as current sheets, and occur in the same regions of parameter space where elevated temperatures are found (Osman et al. 2012b), and also close to identified instability thresholds (Osman et al. 2012a; Maruca et al. 2011). Hybrid-Vlasov and particle in cell simulations of turbulence complement these findings by establishing that kinetic effects are concentrated near regions of strong magnetic stress (Servidio et al. 2012; Drake et al. 2010; Perrone et al. 2013; Wan et al. 2012; Wu et al. 2013; Karimabadi et al. 2013). Here we further investigate this path by exploring a broad range of plasma parameters and establishing a more complex link between temperature anisotropy and turbulence intermittency.

Kinetic plasma turbulence is an incompletely understood problem, and treatments such as linear and quasi-linear

simplifications of the Vlasov–Maxwell equations may provide useful guidance (Davidson 1990). However, for plasmas found to be in a turbulent state, it is not at all obvious whether such simplified models reliably provide a valid description. On both technical and physical grounds, one might question whether linear homogeneous Vlasov theory is sufficient to explain the inhomogeneous plasma dynamics operating near coherent structures. Hence, a strong basis for analyzing the dynamics of such plasmas is provided by direct numerical simulations of plasma kinetic equations, in which the time evolution of the VDF is described self-consistently, and in the absence of particle noise (a crucial point in studying small scale gradients; Haynes et al. 2013). In turbulent systems such as the solar wind (Bruno & Carbone 2005; Sahraoui et al. 2009), it is of crucial relevance to quantify the role of kinetic effects in the turbulent cascade, since this provides a path to explain the energy dissipation mechanisms. Non-Maxwellian features of the VDF represent a direct manifestation of the underlying complex kinetic processes. Here we perform an ensemble of direct numerical simulations of the Hybrid Vlasov–Maxwell (HVM) model (Valentini et al. 2007). We compare results with solar wind datasets from the *Wind* spacecraft, and we investigate the structures that contribute to the local anisotropy observed in the solar wind.

2. ANALYSIS OF SIMULATIONS AND SOLAR WIND DATA

We performed direct numerical simulations of a five-dimensional (two-dimensional (2D) in space; three-dimensional (3D) in velocity space) Vlasov model (Valentini et al. 2007; Servidio et al. 2012) for protons, coupled to a fluid model for electrons. The 2D plane is perpendicular to the mean field $B_0\hat{z}$, and fluctuating vectors are 3D. This 2.5D model is a tradeoff between reality and computational resources, as fully three space dimensions would imply a reduction in the spatial resolution that is essential for turbulence. A 2.5D model may also have an in-plane guide field B_0 (Valentini et al. 2010; Verscharen et al. 2012), where wave activity is favored with respect nonlinear couplings. Therefore, the model we implement makes the opposite approximation. However, since the level of magnetic fluctuations is comparable to the background field, situations where spatial variations occur along the ambient magnetic field are also allowed in our simulations, and the presence of parallel and/or oblique mode-like fluctuations cannot be discarded.

In order to mimic the variability of the solar wind, we vary the plasma beta and also the level of fluctuations $\delta b/B_0$, where δb is the rms fluctuation value. The simulation box is of size $2\pi \times 20d_i$ (d_i is the ion skin depth), with a resolution of 512^2 in the physical space, and a typical resolution of 51^3 in the velocity space. The velocity space resolution is varied for the simulations with smaller plasma beta, where we tested the results by varying the resolution from 51^3 to 81^3. For these parameters, the conservation of the total mass and energy of the system in the simulations is satisfied with typical relative errors of $\simeq 10^{-3}\%$ and $\simeq 10^{-5}\%$, respectively. As described in Servidio et al. (2012), we initialize the turbulence by specifying a band limited Gaussian spectrum of fluctuations, and an isotropic Maxwellian plasma ($T_\perp/T_\parallel = 1$) with uniform temperature. The cross-helicity $\langle \mathbf{v}\cdot\mathbf{b}\rangle$ is initially chosen to be ≈ 0, where $\langle\cdots\rangle$ denotes global average and $\delta b \sim \delta v \sim 1$. The correlation length (energy containing scale) is $\ell \simeq 10d_i$. The range of dynamically accessible scales is a compromise due to a finite simulation size, but it includes both proton kinetic scales and extends into the fluid regime. This class of simulations evolves (Servidio et al. 2012; Greco et al. 2012) by forming a broad band spectrum extending from the correlation scale ℓ to kinetic scales ($<d_i$), implying an effective Reynolds number, as in classical turbulence theory, on the order of $(\ell/d_i)^{4/3}$, while also forming characteristic small scale structures associated with intermittency. Therefore the dynamics appears to be analogous to moderately high ($\gg 1$) Reynolds number strong turbulence.

Table 1
Parameters for the Hybrid Eulerian Vlasov Simulations Discussed in the Text, As Well As Spatial Resolution and Velocity Space Resolution

Run	β	$\delta b/B_0$	Spatial Res.	Velocity Res.	$\tau^*(\Omega_{ci}^{-1})$
V1	0.25	1/3	512^2	81^3	50
V2	0.5	1/3	512^2	81^3	50
V3	1.0	1/3	512^2	51^3	50
V4	1.5	1/3	512^2	51^3	50
V5	2.0	1/3	512^2	51^3	50
V6	5.0	1/3	512^2	51^3	50
V7	0.25	2/3	512^2	81^3	13
V8	1.0	2/3	512^2	51^3	13

Note. The periodic real space domain is $2\pi \times 20d_i$ on a side.

For each simulation we used the data near the time of peak of nonlinear activity τ^* (Servidio et al. 2012), reported in Table 1, in units of the ion cyclotron time Ω_{ci}^{-1}. Following the familiar practice in magnetohydrodynamics (MHD) simulations (Mininni & Pouquet 2009), we estimate this with the time of peak mean square current density. Other analyses (not shown) demonstrate that the conclusions presented here are not sensitive to this choice for times $\sim\tau^*$ or somewhat larger. A scatter plot of temperature anisotropy as a function of the $\beta_\parallel$ is shown in Figure 1 for simulations initialized with $\delta b/B_0 = 1/3$ and with uniform initial plasma beta varying over values $\beta = 0.25, 0.5, 1, 1.5, 2, 5$ (runs V1–V6 in Table 1.) It is apparent that the dynamically evolved data are strongly modulated by the choice of beta and are also spread in temperature anisotropy (note that at $t = 0$, $T_\perp/T_\parallel = 1$). Notably, the resulting distributions resemble the familiar form of those accumulated from years of solar wind data, as in Bale et al. (2009) and Osman et al. (2012a).

In order to further confirm our methodology, a similar analysis is carried out using a large sample of solar wind data, binning the data according to plasma β. We use 17 years of plasma and magnetic field measurements from the *Wind* spacecraft. The Faraday cup instrument in the Solar Wind Experiment (Ogilvie et al. 1995) measures 92*s* resolution proton number density n_p, bulk velocity V_{sw}, and proton temperature. This is separated into parallel $T_\parallel$ and perpendicular $T_\perp$ temperatures by comparison with the local magnetic field from the Magnetic Field Investigation (Lepping et al. 1995). Only solar wind data is used and measurements in the magnetosphere or contaminated by terrestrial foreshock are removed. We also require the uncertainties in the plasma measurements to be less than 10%.

The solar wind dataset is divided into 4-hour non-overlapping datasets (about five correlation lengths). These are sorted into three bins with average values of $\beta = 0.25\pm0.01$, 1.5 ± 0.01, 3 ± 0.01, where all the data falling outside of this range are excluded. When the solar wind data are sorted according to their average β in this way, the distribution of samples migrates systematically toward the right, with increasing spread in $T_\perp/T_\parallel$ for the lower values of $\beta_\parallel$ shown in Figure 1(b). The distributions from the simulations bear strong qualitative resemblance to the trends in the solar wind data. This effect is even more striking given that

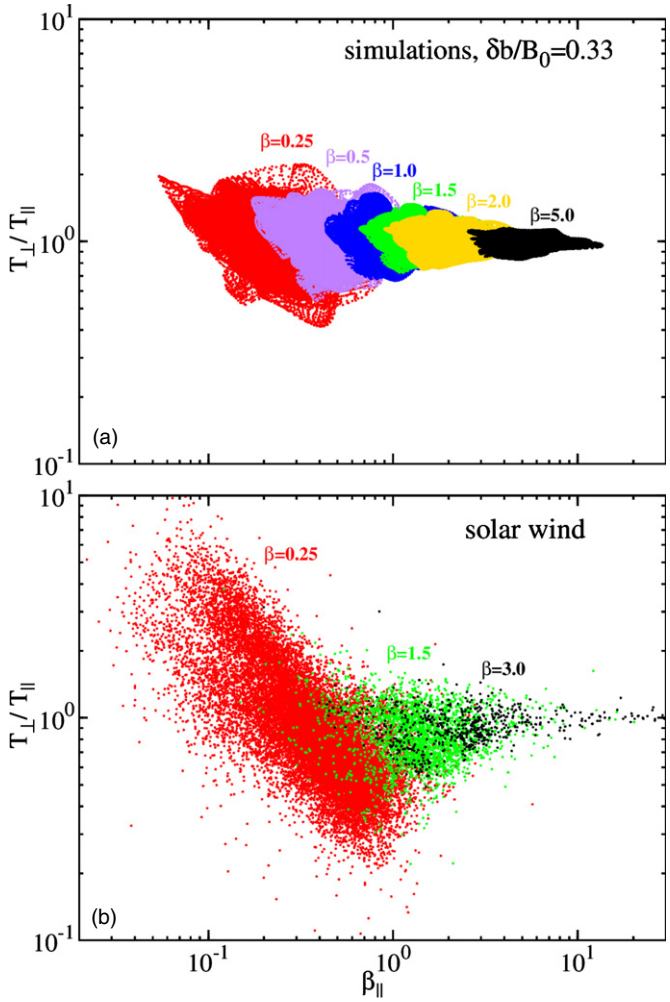

Figure 1. (a) Scatter plot of anisotropy $T_\perp/T_\parallel$ vs. $\beta_\parallel$ for the HVM simulations, performed with $\delta b/B_0 = 0.33$, and varying $\beta = 0.25, 0.5, 1.0, 1.5, 2.0$, and 5.0 (from left to right). (b) Solar wind samples in the same plane, sorted in four-hour samples with average values of $\beta = 0.25$, 1, and 3.

(A color version of this figure is available in the online journal.)

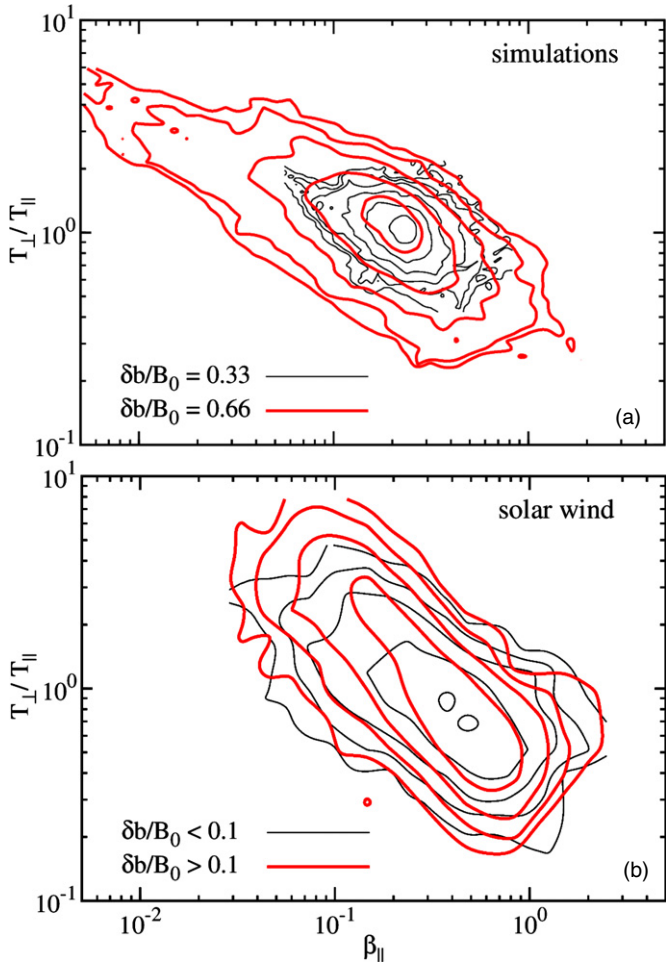

Figure 2. (a) Joint distributions of $T_\perp/T_\parallel$ vs. $\beta_\parallel$, comparing simulations with $(\beta, \delta b/B_0) = (0.25, 1/3)$ (thin-black) and $(0.25, 2/3)$ (thick-red). (b) Samples of solar wind selected for four-hour average values of $\beta = 0.25$, and $\delta b/B_0 < 0.1$ (thin-black), and >0.1 (thick-red).

(A color version of this figure is available in the online journal.)

$\delta b/B_0$ is uncontrolled in the solar wind data. Note that all of the simulations shown in Figure 1 have a (low) initial value of $\delta b/B_0 = 1/3$. The envelope of the simulation distributions is somewhat further away from the reported mirror and firehose instability thresholds discussed in solar wind analyses (Bale et al. 2009; Maruca et al. 2011).

To examine the influence of turbulence level we performed a set of simulations varying the level of fluctuations. In Figure 2 we compare probability density functions (PDFs) of simulation data with $(\beta, \delta b/B_0) = (0.25, 1/3)$ and $(0.25, 2/3)$, namely Run V1 and V7. It is evident that the level of fluctuations, together with the mean plasma beta, strongly influences the distribution of anisotropies in Vlasov turbulence. Similar results have been obtained for the case with $(\beta, \delta b/B_0) = (1, 1/3)$ and $(1, 2/3)$ (not shown here).

A similar analysis conditioning on the turbulence level has been carried out for solar wind, sampling the data for both β and $\delta b/B_0$. See panel (b) of Figure 2. We note that the solar wind comparison with simulation cannot be precise since the values of δb and B_0 as well as other parameters (cross-helicity, Alfvén ratio, etc.) vary almost continuously from sample to sample in the solar wind, while are controlled by the initial data for the relatively few simulations that can be done. However we can clearly discern that the level of fluctuations plays a direct role in spreading the distribution of temperature anisotropies. In particular, a higher turbulence level produces excursions in the distribution to higher values of anisotropy.

A consistent interpretation of the above results is that the turbulent dynamics produces variations in kinetic anisotropies (measured here by $T_\perp/T_\parallel$ and $\beta_\parallel$) even when the global average values are prescribed. Furthermore, when the global average values of β and $\delta b/B_0$ are varied, the dynamical spreading of local anisotropies ventures into different, and sometimes more distant, regions of the parameter space. This effect is observed to be qualitatively similar in the simulations and in the solar wind analysis, keeping in mind of course that the control over parameters is direct in the former case and obtained through conditional sampling in the latter.

This interpretation may be expanded further in the perspective of recent studies that show concentrations of kinetic effects near coherent structures. Elevated temperatures and enhanced kinetic anisotropies are seen near coherent magnetic structures, both in plasma simulations (Servidio et al. 2012; Wan et al. 2012; Wu et al. 2013; Karimabadi et al. 2013) and in solar wind observations (Osman et al. 2011, 2012a, 2012b). One might reason in this way: intermittency is a generic feature of turbulence, leading to coherent structures of increasing sharpness at smaller

scales, the effect growing stronger at higher Reynolds numbers (Sreenivasan & Antonia 1997).As stronger fluctuation amplitude is associated with stronger turbulence (e.g., higher Reynolds number, larger cascade rate), and therefore for a plasma, larger $\delta b/B_0$ should be associated with stronger intermittency and stronger small scale coherent structures. Since coherent structures are connected with kinetic anisotropies, then larger $\delta b/B_0$ should also be connected with stronger anisotropies. This is an alternative to the interpretation put forth previously (Bale et al. 2009) that the fluctuation levels are larger near the parameter space regions with larger anisotropies because instabilities that operate in those regions also act to excite these fluctuations. In the current interpretation the anisotropies are a consequence of turbulence.

At this point we may enquire whether the connection between extremes of kinetic anisotropies and turbulence properties runs deeper still. The connections between coherent structures and kinetic anisotropy that have been established previously (Osman et al. 2012a) have been based on analysis of magnetic fluctuations. However in plasma turbulence dynamical couplings may lead to formation of structure in other fields as well, such as the velocity field and density. It is reasonable to suppose that these too might be sites of enhanced anisotropic kinetic activity. Pursuing this question, here we employ both simulations and solar wind data to explore the possible association of magnetic, density, and velocity gradients with the occurrence of enhanced kinetic effects.

In analogy with previous work on magnetic intermittency (Greco et al. 2008, 2012), we employ a PVI analysis for examination of flow and density gradients. This intermittency measure is given by

$$\Im_f(s) = \frac{|\Delta \mathbf{f}|}{\sqrt{\langle |\Delta \mathbf{f}|^2 \rangle}}, \quad \text{where } \Delta \mathbf{f} = \mathbf{f}(s+\Delta s) - \mathbf{f}(s), \qquad (1)$$

where $\mathbf{f}$ can be the magnetic ($\mathbf{b}$) or velocity ($\mathbf{v}$) vector field, or the scalar density field (n). The brackets $\langle \cdots \rangle$ denote an appropriate time average over many correlation times (the entire simulation box, or the entire solar wind dataset). For the simulations, the variable s is a one-dimensional spatial coordinate, and for the solar wind data it labels the spacecraft time series. The increment lag Δs corresponds to $92s$ time lag for the solar wind data, and is the mesh size for the simulations.

Once the data has been binned in the $(\beta_\parallel, T_\perp/T_\parallel)$ plane, we evaluated the average magnitude of $\Im_f$ in each bin, using all the HVM simulations presented in this work (see Table 1.) As can be seen from Figure 3(a), where $\Im_b$ is shown, the strongest magnetic gradients are found near the threshold regions in the simulations. This is in agreement with the solar wind analysis (Osman et al. 2012a; Servidio et al. 2012), of magnetic coherent structures. This analysis is carried out here on 17 years of solar wind data, and shown in Figure 3(d). Note that varying the increment lag within the inertial range did not qualitatively change the results reported here, which confirm that magnetic gradients are likely playing a role in the observed anisotropy.

We also performed the same analysis for the velocity field, obtaining $\Im_v$, which is a surrogate for the vorticity of the flow. It is immediately clear, as shown in Figure 3(b), that intermittency of the velocity is also strongly correlated to kinetic anisotropy. Furthermore, the signatures are once again found near the boundaries of the characteristic anisotropy plot. Finally, panel (c) of Figure 3 reports the same analyses for $\Im_n$, an indicator of intermittent structure in the density field. The density results qualitatively resemble both the magnetic and velocity field cases. In each case we repeated the same analysis for the data in the solar wind, as shown in panels (d)–(f) of Figure 3. In each case, for the magnetic field, the velocity field, and the density field, the shape of the distributions are qualitatively similar in the simulation and solar wind datasets. Furthermore, the highest average values of PVI are found in each case near the extremal regions of the parameter space and these values are comparable in the simulations and solar wind data. Note that due to the limited number of available simulations, those distributions do not experience parameter excursions as great as those of the solar wind data.

3. CONCLUSIONS AND DISCUSSION

To summarize, the results of nonlinear hybrid-Vlasov simulations in five dimensions show that: (1) the initially controlled average plasma beta and fluctuation level leads dynamically to a spread in the $(\beta_\parallel, T_\perp/T_\parallel)$ plane, reminiscent of solar wind populations in the same parameter plane; (2) simulations with moderate variations of average β and $\delta b/B_0$ lead to fuller coverage of the $(\beta_\parallel, T_\perp/T_\parallel)$ plane, a tendency that is reproduced by conditional sampling of a large number of solar wind datasets; (3) that the simulations naturally lead to stronger $\delta b/B_0$ near the boundaries of the distribution; and (4) that the extreme regions of the distribution of points in the $(\beta_\parallel, T_\perp/T_\parallel)$ plane also show enhanced values of magnetic field gradients, velocity shears, and density gradients. These features, corroborated here by observations, point to a strong connection between kinetic anisotropies and intermittent turbulence.

Evidently the broad distribution of solar wind samples in the $(\beta_\parallel, T_\perp/T_\parallel)$ plane, can be explained by the variability inherent in the turbulent evolution of a collisionless plasma. This result complements prior findings concerning this distribution: the trend toward lower anisotropy and higher beta is associated with expansion (Hellinger et al. 2006; Matteini et al. 2007; Hellinger & Trávníček 2008). Arguments have been made that the extreme excursions of parameters are controlled by instabilities (Kasper et al. 2002; Hellinger et al. 2006; Bale et al. 2009; Maruca et al. 2011), which may be localized near coherent structures (Veltri 1999; Greco et al. 2008; Servidio et al. 2012; Osman et al. 2012a). Here we have seen that turbulence drives the system toward the conditions of instability, although the 2.5D system employed is not always well suited to follow the evolution of those linear instabilities. Taken together, a relatively complete picture begins to emerge of the physics operating in beta-parallel and temperature anisotropy.

The current analyses of Vlasov simulations and solar wind data point toward the same conclusions, namely that in plasma turbulence there is a strong link between intermittent structures and kinetic anisotropy. The multiple analyses presented here suggests that the intermittent structures, in the magnetic field, the velocity field, and the density, may be central ingredients in sustaining the observed kinetic anisotropies. Even if structures may locally be found in near-equilibrium conditions, in the absence of collisions such configurations might require a certain amount of temperature anisotropy (Mikhailovskii 1974). The results presented here are complementary to MHD test-particle results that showed perpendicular proton anisotropy developing near current sheets (Dmitruk et al. 2004) due to a betatron-like mechanisms or to stochastic mechanisms (Xia et al. 2013). Calculations of local kinetic equilibria near coherent structures may help to explain both parallel and perpendicular heating mechanisms. Other effects, such as non-gyrotropic distributions,

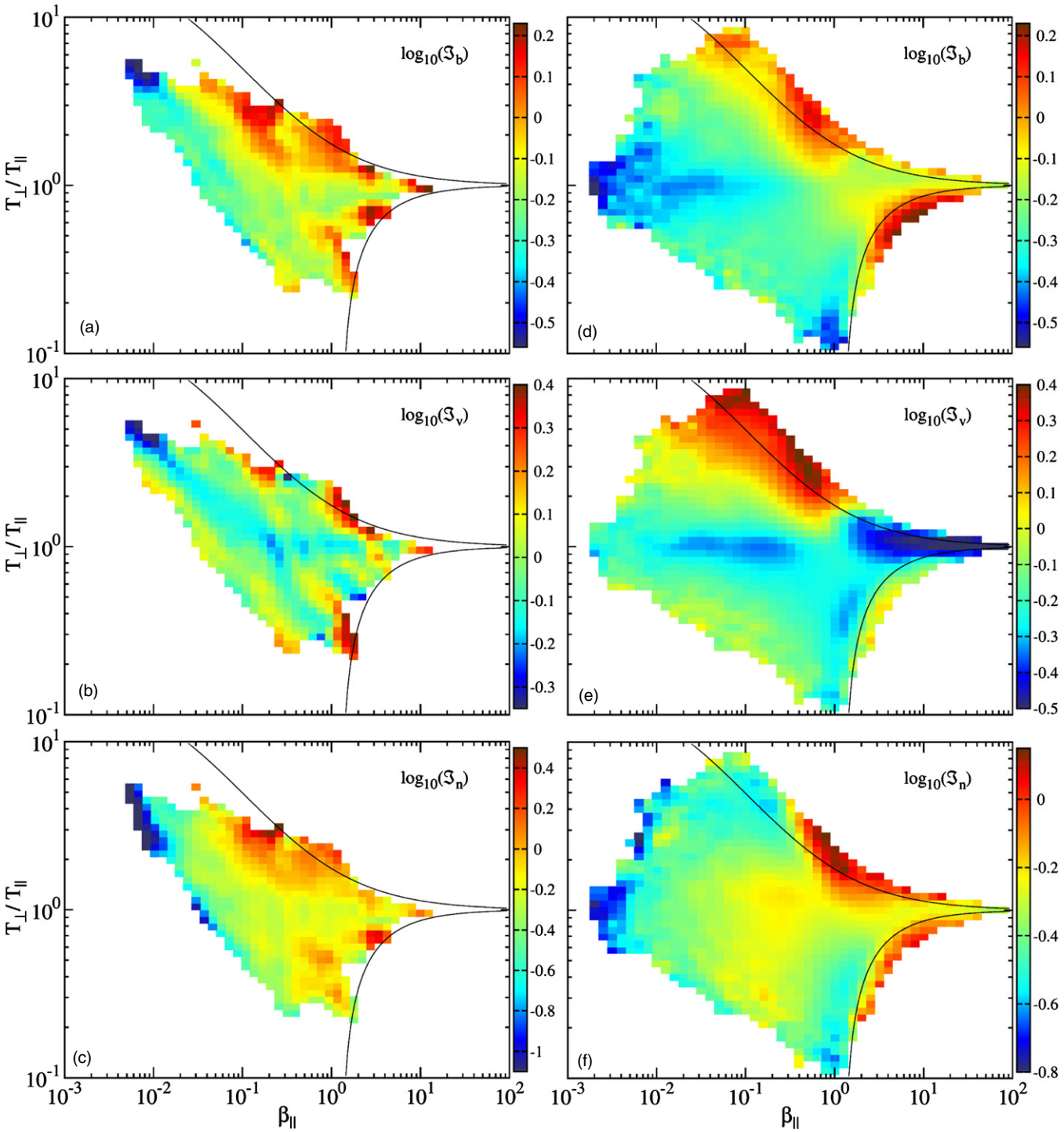

Figure 3. Average $\Im_f$ in the anisotropy–$\beta_\parallel$ plane for the ensemble of simulations: $\Im_b$ (a), $\Im_v$ (b), and $\Im_n$ (c). Same for the solar wind, in panels (d)–(e). In each panel, dashed curves indicate theoretical growth rates for the mirror ($T_\perp/T_\parallel > 1$) and the oblique firehose ($T_\perp/T_\parallel < 1$) instability.
(A color version of this figure is available in the online journal.)

and the presence of non-null third- and fourth-order moments of the VDFs may play other interesting roles in the dynamics (Servidio et al. 2012). The departure from simple bi-Maxwellian distributions represents a limitation of the comparison between simulations and observations, and will be investigated in future works.

Effects not examined here may also be important in controlling kinetic anisotropies. For example, 3D effects may be important, as in that case both low frequency couplings and MHD-type wave modes (Verscharen et al. 2012) contribute on an equal basis. The kinetic response of electrons, not explored here, may be interesting as well and has been recently implicated in producing coherent structures (see, e.g., Karimabadi et al. 2013). Further and more elaborate simulations and analysis will be required to incorporate all of these effects in a single study. However, we suspect that greater realism will show additional effects while the basic features we have described will persist: intermittent turbulence and coherent structures have

a significant influence on the development of kinetic effects in a low collisionality plasma such as the solar wind.

This research was partially supported by the Turboplasmas project (Marie Curie FP7 PIRSES-2010-269297), POR Calabria FSE 2007/2013, the NASA Magnetosphere Multiscale Mission Theory and Modeling program NNX08AT76G, UK STFC, the Solar Probe Plus ISIS project, the NSF SHINE (AGS-1156094) and Solar Terrestrial (AGS-1063439) Programs, and MIUR (PRIN 2009, 20092YP7EY). Numerical simulations were performed on the FERMI supercomputer at CINECA (Bologna, Italy) within the European project PRACE Pra04-771.

REFERENCES

Bale, S. D., Kasper, J. C., Howes, G. G., et al. 2009, PhRvL, 103, 211101
Bruno, R., & Carbone, V. 2005, LRSP, 2, 4
Davidson, R. C. 1990, Physics of Nonneutral Plasmas (Redwood City, CA: Addison-Wesley)
Dmitruk, P., Matthaeus, W. H., & Seenu, N. 2004, ApJ, 617, 667
Drake, J. F., Opher, M., Swisdak, M., & Chamoun, J. N. 2010, ApJ, 709, 963
Gary, S. P. 1993, Theory of Space Plasma Microinstabilities (Cambridge: Cambridge Univ. Press)
Greco, A., Chuychai, P., Matthaeus, W. H., Servidio, S., & Dmitruk, P. 2008, GeoRL, 35, L19111
Greco, A., Valentini, F., Servidio, S., & Matthaeus, W. H. 2012, PhRvE, 86, 066405
Haynes, C. T., Burgess, D., & Camporeale, E. 2013, arXiv:1304.1444
Hellinger, P., & Trávníček, P. M. 2008, JGR, 113, A10109
Hellinger, P., Trávníček, P., Kasper, J. C., & Lazarus, A. J. 2006, GeoRL, 33, L09101
Karimabadi, H., Roytershteyn, V., Wan, M., et al. 2013, PhPl, 20, 012303
Kasper, J. C., Lazarus, A. J., & Gary, S. P. 2002, GeoRL, 29, 20
Lepping, R. P., Acũna, M. H., Burlaga, L. F., et al. 1995, SSRv, 71, 207
Marsch, E. 2006, LRSP, 3, 1
Marsch, E., Ao, X.-Z., & Tu, C.-Y. 2004, JGR, 109, A04102
Marsch, E., Schwenn, R., Rosenbauer, H., et al. 1982, JGR, 87, 52
Maruca, B. A., Kasper, J. C., & Bale, S. D. 2011, PhRvL, 107, 201101
Matteini, L., Landi, S., Hellinger, P., et al. 2007, GeoRL, 34, L20105
Matthaeus, W. H., & Montgomery, D. 1980, NYASA, 357, 203
Mikhailovskii, A. B. 1974, Theory of Plasma Instabilities, Vol. 2, Instabilities in an Inhomogeneous Plasma (New York: Plenum)
Mininni, P. D., & Pouquet, A. 2009, PhRvE, 80, 025401
Ogilvie, K. W., Chornay, D. J., Fritzenreiter, R. J., et al. 1995, SSRv, 71, 55
Osman, K. T., Matthaeus, W. H., Greco, A., & Servidio, S. 2011, ApJL, 727, L11
Osman, K. T., Matthaeus, W. H., Hnat, B., & Chapman, S. C. 2012a, PhRvL, 108, 261103
Osman, K. T., Matthaeus, W. H., Wan, M., & Rappazzo, A. F. 2012b, PhRvL, 108, 261102
Parker, E. N. 1988, ApJ, 330, 474
Perrone, D., Valentini, F., Servidio, S., Dalena, S., & Veltri, P. 2013, ApJ, 762, 99
Sahraoui, F., Goldstein, M. L., Robert, P., & Khotyaintsev, Yu. V. 2009, PhRvL, 102, 231102
Servidio, S., Valentini, F., Califano, F., & Veltri, P. 2012, PhRvL, 108, 045001
Sreenivasan, K. R., & Antonia, R. A. 1997, AnRFM, 29, 435
Valentini, F., Califano, F., & Veltri, P. 2010, PhRvL, 104, 205002
Valentini, F., Trávníček, P., Califano, F., Hellinger, P., & Mangeney, A. 2007, JCoPh, 225, 753
Veltri, P. 1999, PPCF, 41, A787
Verdini, A., Velli, M., Matthaeus, W. H., Oughton, S., & Dmitruk, P. 2010, ApJL, 708, L116
Verscharen, D., Marsch, E., Motschmann, U., & Müller, J. 2012, PhPl, 19, 022305
Wan, M., Matthaeus, W. H., Karimabadi, H., et al. 2012, PhRvL, 109, 195001
Wu, P., Perri, S., Osman, K., et al. 2013, ApJL, 763, L30
Xia, Q., Perez, J. C., Chandran, B. D. G., & Quataert, E. 2013, ApJ, 776, 90